(Text of Invited Talk at Symposium of Shell-Model Investigations of Medium-Weight Nuclei, University of Tokyo, September 4, 1977)

CONF-770977--1

SHELL-MODEL ORIGINS OF COLLECTIVE EFFECTS IN LIGHT- AND MEDIUM-WEIGHT NUCLEI

J. B. McGrory
Oak Ridge National Laboratory*
Oak Ridge, Tennessee 37830

NOTICE
This report was prepared as an account of work sponsored by the United States Government. Neither the United States nor the United States Energy Research and Development Administration, nor any of their employees, nor any of their contractors, subcontractors, or their employees, makes any warranty, express or implied, or assumes any legal liability or responsibility for the accuracy, completeness or usefulness of any information, apparatus, product or process disclosed, or represents that its use would not infringe privately owned rights.

The two generic models for the description of nuclear phenomena are the microscopic shell model and the collective model. The successes of both are well documented. In the lower half of the s-d shell there are a number of nuclei whose spectra contain states which appear to constitute rotational bands. For these nuclei, complete shell-model calculations are possible in which a ^{16}O core is assumed, and valence particles are restricted to the 0s,1d shell. These calculations reproduce the observed rotational features. Thus, the rotational behavior is produced by the motion of only the valence particles. The particles in the ^{16}O core enter only through the single-particle energies and the renormalization of the residual one-body (effective charges) and two-body interaction. Recently, Iachello and Arima have proposed[1] an interacting boson model (IBM) which is applicable in the transitional and deformed region, which appears capable of describing both rotations and vibrations, and which implicitly assumes that this collective behavior can be generated by the motion of relatively few valence nucleons. In this brief report I would like to discuss two independent investigations which illustrates that there appear to be interesting collective features in some f-p shell nuclei which are

*Research sponsored by the U. S. Energy Research and Development Administration under contract with the Union Carbide Corporation.

MASTER

DISTRIBUTION OF THIS DOCUMENT IS UNLIMITED

By acceptance of this article, the publisher or recipient acknowledges the U.S. Government's right to retain a non - exclusive, royalty - free license in and to any copyright covering the article.

generated from the motion of valence nuclei, and that the structure of the states in question is consistent with the philosophy of the IBM. Finally, I will discuss some further investigations of shell-model wave functions in the s-d shell and light f-p shell nuclei which also offer some support to the IBM model. I should stress the preliminary nature of these results. Most of what I'll discuss is mostly suggestive and demands much more detailed investigation.

The first calculations I'd like to discuss are shell-model calculations in the mass region around A = 50-60. The states of principle interest are the so-called YRAST levels in these nuclei; i.e., the lowest state of each J in a given spectrum. The model[2] is an often-used one. An inert ^{48}Ca core is assumed, protons are restricted to the $f_{7/2}$ shell, and neutrons occupy the $p_{3/2}$, $f_{5/2}$, and $p_{1/2}$ orbits. Single neutron energies suggested by the observed ^{49}Ca spectrum are used. The two-body interaction is taken from the literature from studies of the Ni isotopes and the N=29 nuclei. A similar model with a somewhat different and more accurate interaction has been used by Horie and Ogawa in other studies[3] in this region. I have calculated the spectra of isotopes of Ti, V, Cr, Mn, Fe, and Co with from 2-9 neutrons. The N=30 isotopes of these nuclei were studied[2] some years ago with this model with a high degree of success. Recently the model has been used[4] by Mateja et al. to study the ^{55}Mn(t,p)^{57}Mn reaction. The calculated two-particle strengths very accurately mirror experiment, including considerable L-mixing in a number of transitions. More recently, Nathan et al.[5] have studied the high-spin states in a number of these nuclei in (heavy ion, xn) reactions. In general, the predicted spectra are in reasonable agreement with the spectra suggested by experiment. There is a tendency for the calculated levels to be too high with respect to experiment by 200-300 keV. This is the case for

all the N=30 nuclei. The consistent defect in the N=30 nuclei is largely corrected by the Horie-Ogawa interaction. The main point is that the theory-experiment agreement is good enough in enough cases to have a high degree of confidence in the calculations, and, in particular, to discuss properties of levels for which experimental analogs are not yet known.

I'd like to point first to a rather consistent feature in many of the calculated spectra. In Figs. 1 and 2, the calculated spectra for $^{54,56}Cr$, $^{56,58,60}Fe$, $^{55,57}Mn$, and $^{57,59}Fe$ are shown. There is a doublet structure of the YRAST levels which becomes more pronounced as the number of neutrons is increased. For the odd nuclei, this structure is suggestive of some of the spectra resulting from the aligned coupling schemes[6] introduced by Stephens and Simon to account for backbending phenomena in heavier nuclei.

I have developed a backbending plot for the YRAST levels of ^{60}Fe. The result is shown in Fig. 3. The familiar S-shaped curve is clearly evidenced. Similar curves for ^{56}Fe and ^{58}Fe, not shown here, do not have this smooth behavior. I have looked at the quadrupole operator observables for these three nuclei. In Table 1 the quadrupole moments and B(E2)-values for YRAST states with even J for ^{56}Fe, ^{58}Fe, and ^{60}Fe are shown. For ^{56}Fe, the shape of the nucleus starts oblate, goes prolate at the 6^+, and returns to oblate for the 8^+ and 10^+. For ^{58}Fe, the nucleus is oblate up to the $J=6^+$ state, and prolate for the 8^+ and 10^+. For ^{60}Fe, the shape transition occurs between the $J=4^+$ and $J=6^+$ states. This shape transition is reflected in the B(E2)-values. There is consistently a diminution of the B(E2)-value where a shape change occurs.

This leads to a rather neat model of the structure, ^{60}Fe. The nucleus displays a classic backbending behavior, and the backbending occurs as a result of the crossing of two rotational bands. This "collective" picture is

not so clear in ^{56}Fe or ^{58}Fe. Thus, the collectivity appears as more neutrons are added. Some preliminary results similar to these for ^{56}Fe were reported by Bendjaballah et al.[7] The measured lifetimes for states in ^{56}Fe were accounted for by the Horie-Ogawa calculations of ^{56}Fe. In particular, the lifetime of the first 6^+ was much longer than for the lower-spin states.

These results are also consistent with the results of Sharma[8] who studied the Fe isotopes in a Hartree-Fock-Bogolubov calculation. He found that the prolate and oblate solutions lay close to each other in energy, as is suggested by the band-crossing in the shell-model calculations.

It is worth noting that the B(E2)'s between the high-spin prolate states in ^{60}Fe are much stronger than in ^{58}Fe. It would obviously be interesting to verify this pattern.

Again, I stress the preliminary nature of these results, and that the collective behavior is only suggestive. It does appear to be another example where collective behavior is introduced in the motion of relatively few valence nuclei.

This is a basic premise of the IBM, as will be discussed by Igal Talmi later in this symposium. They attempt to describe the transition from vibrational to rotational behavior in one series of nuclei as one goes from a closed shell to the middle of the shell and on to the end of the shell. Very crudely, they say that the neutron (proton) states of valence nuclei can be constructed from two basic two-particle "bosons", a J=0 and a J=2 boson. Thus, four identical-particle states result from coupling two of these bosons. The collective behavior then evolves from the coupling of these proton and neutron boson states through the n-p interaction. Their picture of ^{56}Fe would be that it results from coupling two-proton hole "bosons" with J = 0 and J = 2 to two-neutron-particle bosons with J = 0 and J = 2. One might reasonably approximate these

bosons by the lowest $J=0^+$ and $J=2^+$ states in ^{54}Fe and ^{58}Ni, and say that the 2^+ states in ^{56}Fe are mixtures of the states $0^+(^{54}Fe) \times 2^+(^{58}Ni)$, $2^+(^{54}Fe) \times 0^+(^{58}Ni)$, and $2^+(^{54}Fe) \times 2^+(^{58}Ni)$. Bhatt et al. did analyze the ^{56}Fe wave functions in a model identical to the one discussed above. They found that the ground state band of ^{56}Fe is indeed dominated by these three states. For instance, the $J=2^+$ state is more than 95% in these three states.

Several years ago, I developed some programs in collaboration with L. B. Hubbard to carry out shell-model calculations in a truncated space, where the truncation scheme was chosen on grounds very similar to the foundations of the IBM model. Some of the calculations we did in the course of developing the program are of interest with respect to the interacting boson model, and I'd like to discuss them in the remainder of this report.

The effective residual shell model Hamiltonian can be written in neutron-proton formalism, in obvious notation,

$$H = H_{nn} + H_{pp} + H_{pn}.$$

In many shell model cases, it is possible to solve the shell-model calculation exactly for the neutrons and protons separately. Thus, the following equations

$$H_{nn}|\psi_n^i\rangle = E_n'|\psi_n^i\rangle$$

$$H_{pp}|\psi_p^j\rangle = E_p^j|\psi_p^j\rangle$$

define a complete set of states in the neutron and proton spaces separately. The direct product space

$$|\psi_{ij}\rangle = |\psi_n^i\rangle \times |\psi_p^j\rangle$$

forms a complete space for the full shell model space. For example, in a s-d shell-model calculation in which the ^{16}O core is inert, and particles

are limited to the s-d shell, the states in ^{20}Ne can be expanded as linear combinations of states in ^{18}O coupled to states in ^{18}Ne. There are 14 independent two-particle states in ^{18}O with fixed J in this model, so there are at most 256 states in ^{20}Ne in this representation for any given J. In some cases, it may be possible to select a subset of states in the proton space and a subset of states in the neutron space, such that the states in the direct product space of these two subspaces form the dominant part of the wave functions of the low-lying states in the coupled neutron-proton system. The hope is that it is possible to find a truncated space which is large enough to adequately describe low-lying states, but small enough to lead to a tractable calculation in those cases where the full shell-model calculation is unreasonably large. We have developed programs to perform such calculations. As a first test of the program, we looked at some s-d shell and f-p shell nuclei where the exact shell model diagonalization in the complete space is possible, so that we could study the effects of space truncation. In this talk, I'd like to present and discuss results for ^{20}Ne and ^{44}Ti. The ^{20}Ne calculation is the one described above. For ^{44}Ti, an inert ^{40}Ca core is assumed, and the valence particles are restricted to the 0f-1p shell. In both cases, Kuo-Brown matrix elements of the effective Hamiltonian were used, but the types of results I'll discuss are unlikely to depend on the choice of the interaction. The single-particle energies used were those suggested by the spectra of ^{17}O and ^{41}Ca. The complete shell-model calculations were made with the Oak Ridge-Rochester shell model programs.

Figure 4 presents some results of energy level calculations for ^{20}Ne. The left-most spectrum is that resulting from the complete $(sd)^4$ calculation. The numbers under each of the other spectra indicate the space truncation used in the two-neutron and two-proton parts of the space. Thus, the

right-most spectrum is labeled 3 × 3. This means the lowest three states in ^{18}O (i.e., the lowest $J=0^+$, 2^+, and 4^+ states), and the same lowest three states in ^{18}Ne were included in the model space. In the spectrum labeled 6 × 6, the lowest six states in each space were included in the calculation, and so on. Figure 5 shows analogous results for ^{44}Ti. The results for the two calculations are very similar. To obtain a spectrum which is qualitatively similar to the spectrum of the exact calculation, it is necessary only to include the lowest two states of even J, i.e., in ^{20}Ne, include the lowest two $J=0^+$, 2^+, and 4^+ states of ^{18}O and ^{18}Ne. The improvement which results from adding more states is mostly one of trimming up quantitative agreement.

In Tables 2 and 3 the calculated B(E2)-values for transitions between low-lying states in ^{20}Ne and ^{44}Ti are presented. Effective charges ε_p = 1.5e and ε_n = 0.5e have been used in both model spaces. Here again, the qualitative structure of the transition strengths among low-lying states is reproduced in the space with the two lowest $J=0^+$, 2^+, 4^+, etc. states in both ^{20}Ne and ^{44}Ti. The absolute strengths are surprisingly well accounted for by the truncated calculations. A single small increase of the effective charge would give rather accurate agreement with the exact calculations. For the ground state band transitions, the calculation in the smallest spaces really account for the relative strength rather well. The same is not true for the states outside the ground state band. In ^{20}Ne in the 3 × 3 space, the cross-over transition from the second 2^+ to the ground state is almost as strong as the transition to the second 0^+ state. In the exact calculations, the cross-over transition is strongly suppressed. When the second $J=0^+$, 2^+, and 4^+ states are included to produce the 6 × 6 results, the picture is dramatically improved. Entirely analogous results exist for ^{44}Ti. The qualitative

features of all the B(E2)'s shown in Table 3 for the complete space shell-model calculations are reproduced in the 8 × 8 space.

I have looked at the structure of some of the wave functions in ^{20}Ne and ^{44}Ti. In Table 4, an analysis of the wave functions of the two lowest $J=0^+$ states in ^{20}Ne is shown. In this table J_1 and J_2 refer to the J of the two-particle states in the proton and neutron spaces separately. The subscripts identify the proton or neutron states as the first, second, etc. states of that spin. The a_{ij} is the admixture of each of these basis states in the first and second 0^+ state in ^{20}Ne, respectively. Results are shown for the 3 × 3, 6 × 6, and exact (14 × 14) spaces. The percentage figures at the lower part of the table are the percent of the exact wave functions that are in the states in the 3 × 3 and 6 × 6 spaces, respectively (i.e., 76% of the exact 0^+ ground state wave function consists of states which involve only the lowest $J=0^+$, 2^+, and 4^+ states in ^{18}O and ^{18}Ne). The figures labeled overlap indicate how much the part of the exact wave function in the 3 × 3 and 6 × 6 spaces resemble the corresponding eigenstates which result from diagonalization in only the smaller space. Thus, if we consider only the first three components in the exact wave function for the lowest $J=0^+$ space in ^{20}Ne, renormalize these "three component wave functions", and overlap it with the lowest 0^+ state in the 3 × 3 space, the overlap is > 0.999. The implications of this analysis are entirely consistent with the results of the calculations of energies and E2 observables. The 3 × 3 calculation gives a reasonable description of the exact calculations. The case for the excited $J=0^+$ is a different story. Only 16% of the complete wave function of this state is in the 3 × 3 space. The 6 × 6 wave function, however, is quite similar to the 6 × 6 part of the complete wave functions, and 91% of the complete wave function is in the 6 × 6 space.

It is interesting to note the structure of the ground state wave function. Ones intuition might suggest the largest component in the ^{20}Ne ground state would be the state which results from coupling the ground states of ^{18}O and ^{18}Ne. In fact, in the complete shell model wave function, the largest amplitude is for the coupling of the lowest 2^+ states in ^{18}O and ^{18}Ne. This results from the important role of the neutron-proton interaction in generating the collective nature of the neutron-proton systems. The strong admixture of the two 2^+ states can be shown to occur because of large $0^+ \rightarrow 2^+$ matrix elements of the mass quadrupole operator in ^{18}O and ^{18}Ne. Thus, the strong collectivity in ^{20}Ne occurs because of a coherent mixing of strong quadrupole collectivity in the separate neutron and proton spaces.

A similar analysis of the wave functions of the lowest $J=0^+$ states in ^{44}Ti is shown in Table 5. In this case, I have not done the complete space calculation for ^{44}Ti in this neutron-proton representation. Thus, in Table 5, a comparison is made of the lowest two $J=0^+$ in the 4×4 and 8×8 spaces. The general results are the same as in the case for ^{20}Ne. The structure of the wave function of the lowest $J=0^+$ state in the 4×4 space is very similar to the part of the 8×8 wave function that is in the 4×4 space. For the second 0^+ state, only 20% of the 8×8 wave function is in the 4×4 space.

The IBM model would treat the ground state bands of ^{20}Ne and ^{44}Ti as mixtures of a $J=0^+$ and $J=2^+$ neutron "boson" to a $J=0^+$ and $J=2^+$ proton boson. The results shown here offer some support to the assumptions of their model. These calculations show that the ground state band properties of ^{44}Ti and ^{20}Ne are rather well reproduced by the smallest calculations. In ^{20}Ne, 93% of the ground state 0^+ state consists of only the lowest 0^+ and 2^+ neutron and proton states. In ^{44}Ti, 92% of the ground state is in the analogous 0^+ and 2^+ spaces. In the lowest 2^+ of ^{44}Ti in the 4×4 model space, 82% of the wave function

is involved in the 0^+ and 2^+ two-particle states.

There is a disagreement for the lowest 4^+ state in ^{44}Ti. Only 30% of this function is in the $0^+ + 2^+$ "boson" space. It is a possibility that the spaces dealt with here are too small and simple, and that the IBM will be better for the more complicated wave function. Calculations involving up to four neutrons and protons are being started.

The calculations described here suggest that this approach might be a useful truncation scheme for doing calculations where complete shell-model calculations are intractable. These test cases involve neutrons and protons in the same orbits which could maximize the effects of the neutron-proton interaction. But the approach in a sense assumes the n-p interaction is a perturbation. In cases of heavier nuclei, neutrons and protons are in different orbits, and effects of H_{np} may be somewhat weaker, and this approach may be better. Also these calculations in this scheme may be a useful complement to the development of the IBM models.

List of References

1. F. Iachello and A. Arima, Phys. Lett.
2. J. B. McGrory, Phys. Rev. 160, 915 (1967).
3. H. Horie and K. Ogawa, Nucl. Phys. A216, 407 (1973).
4. J. F. Mateja, C. P. Browne, C. E. Moss, and J. B. McGrory, Phys. Rev. C15, 1708 (1977).
5. A. M. Nathan, J. W. Olness, E. K. Warburton, and J. B. McGrory, Phys. Rev. C16, 192 (1977).
6. F. S. Stephens, Revs. Mod. Phys. 47, 43 (1975).
7. N. Bendjaballah, J. Delaunay, T. Nomura, and H. J. Kim, Phys. Rev. Lett. 36B, 1536 (1976).
8. S. K. Sharma, Phys. Lett. 52B, 299 (1974).
9. K. H. Bhatt, S. P. Pandya, and J. B. McGrory, Nucl. Phys. A234, 301 (1974).

Table 1. E2-Operator in Even Fe Isotopes
(ε_p = 1.2e, ε_n = 1.9e)

J	^{56}Fe	Q(efm^2) ^{58}Fe	^{60}Fe
2	-37	-41	-45
4	-43	-35	-53
6	56	-35	23
8	-13	74	54
10	- 6	38	69
12		-	-

$J_i \rightarrow J_f$		$B(E2)_{i\rightarrow f}$	(e^2fm^4)
2-0	358	536	551
4-2	456	594	724
6-4	57	628	232
8-6	27	25	358
10-8	87	43	400
12-10		67	270

Table 2. Calculated B(E2)-Values for Selected E2-Transitions Between Low-Lying States in ^{20}Ne in Various Model Spaces

		B(E2) e^2fm^4 (ε_p = 1.5e, ε_n = 0.5e)		
J_i J_f	Space	3 × 3	6 × 6	Full
$2_1 \rightarrow 0_1$		182	222	241
$4_1 \rightarrow 2_1$		410	488	537
$6_1 \rightarrow 4_1$		506	571	635
$8_1 \rightarrow 6_1$		404	445	529
$2_2 \rightarrow 0_1$		7.3	0.1	0.4
$2_2 \rightarrow 0_2$		12.3	66	81

Table 3. Calculated B(E2)-Values for Selected E2-Transitions Between Low-Lying States in ^{44}Ti in Various Model Spaces

J_i	J_f		B(E2) e^2fm^4 (ε_p=1.5e, ε_n=0.5e)			
		Space	4 × 4	8 × 8	11 × 11	$(fp)^4$
2_1	0_1		69	83	90	96
4_1	2_1		83	104	115	122
6_1	4_1		65	81	96	101
8_1	6_1		60	73	78	79
2_2	0_1		0.1	3.0	2.0	2.6
2_2	2_1		60	115	117	128
4_2	2_1		5	0.8	0.4	0.02
2_2	4_1		1.2	14	17	14
4_2	4_1		22	57	61	58
4_2	2_2		22	58	66	69
4_2	6_1		0.7	21	19	19

Table 4. Structure of Lowest Two $J=0^+$ States in ^{20}Ne in Various Truncated Spaces, as Described in the Text

		0_1^+			0_2^+		
J_1	J_2	a_{ij}(3 × 3)	a_{ij}(6 × 6)	a_{ij} Full	a_{ij}(3 × 3)	a_{ij}(6 × 6)	a_{ij} Full
0_1	0_1	0.693	0.618	0.580	0.719	0.308	0.282
2_1	2_1	0.668	0.655	0.603	-0.669	-0.158	-0.175
4_1	4_1	0.269	0.250	0.240	-0.189	0.198	0.213
0_2	0_2					-0.122	-0.118
2_2	2_2						
4_2	4_2		0.100	0.121		0.100	0.103
$0_1(0_2)$	$0_2(0_1)$		0.100			-0.456	-0.437
$2_1(2_2)$	$2_2(2_1)$		0.130	0.129		-0.416	-0.377
$4_1(4_2)$	$4_2(4_1)$		0.170	0.190		0.164	0.176
Overlap		0.999	0.986		.906	.998	
% in full		76	88		16	91	

Table 5. Structure of Lowest Two $J=0^+$ States in ^{44}Ti in 4 × 4 and 8 × 8 Spaces. The basis state $|\psi_1 \times \psi_2, J=0\rangle$ is described in Columns 1 or 2. Column 3 shows the amplitude, a_i, for that basis state in the wave function. All amplitudes are shown for the 4 × 4 wave functions. The amplitudes of the same 4 × 4 states are listed in the 8 × 8 wave function, plus all amplitudes $|a_i| > 0.1$. The last two entries, % and overlap, are explained in the text.

ψ_1	ψ_2	0_1^+		0_2^+	
		a_i, 4 × 4	a_i, 8 × 8	4 × 4	8 × 8
0_1	0_1	.806	.760	-.323	-.163
2_1	2_1	.520	.516	.786	.320
4_1	4_1	.245	.251	-.440	-.244
6_1	6_1	.142	.156	-.288	-.127
$0_1(0_1)$	$0_2(0_2)$				.237
$2_1(2_2)$	$2_2(2_1)$				-.549
$4_1(4_2)$	$4_2(4_1)$				.193
2_2	2_2				-.136
4_2	4_2				-.106
% (4 × 4) in (8 × 8)			93%		20%
Overlap			.9995		.973

FIGURE CAPTIONS

Figure 1. Calculated spectra of YRAST levels in odd-even nuclei.

Figure 2. Calculated spectra of YRAST levels in even-even nuclei.

Figure 3. Backbending plot of $2^+ \rightarrow 12^+$ YRAST states in ^{60}Fe.

Figure 4. Spectra of ^{20}Ne in various truncated spaces, as discussed in the text.

Figure 5. Spectra of ^{44}Ti in various truncated spaces, as discussed in the text.

ORNL-DWG 77-13214

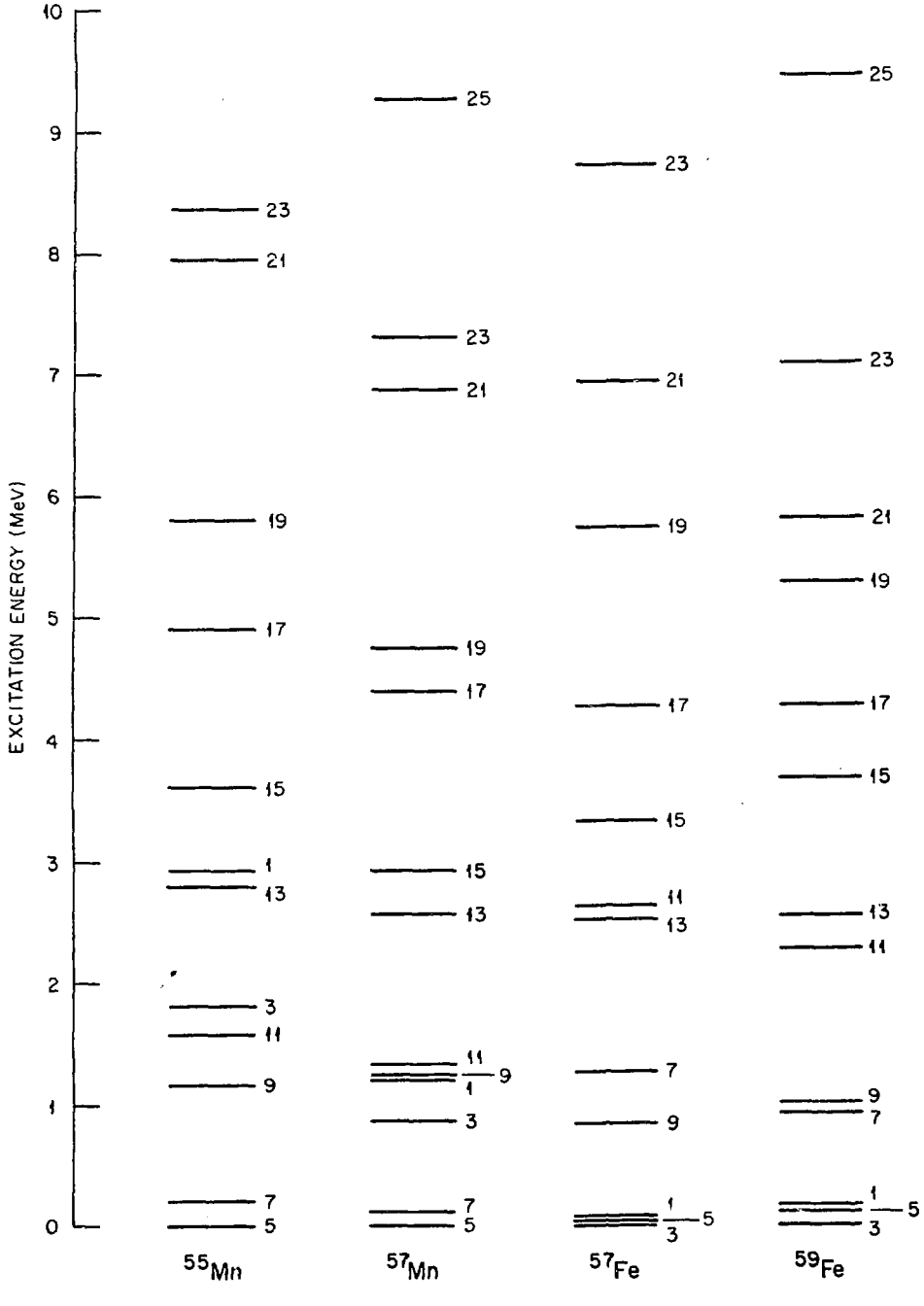

ORNL-DWG 77-13213

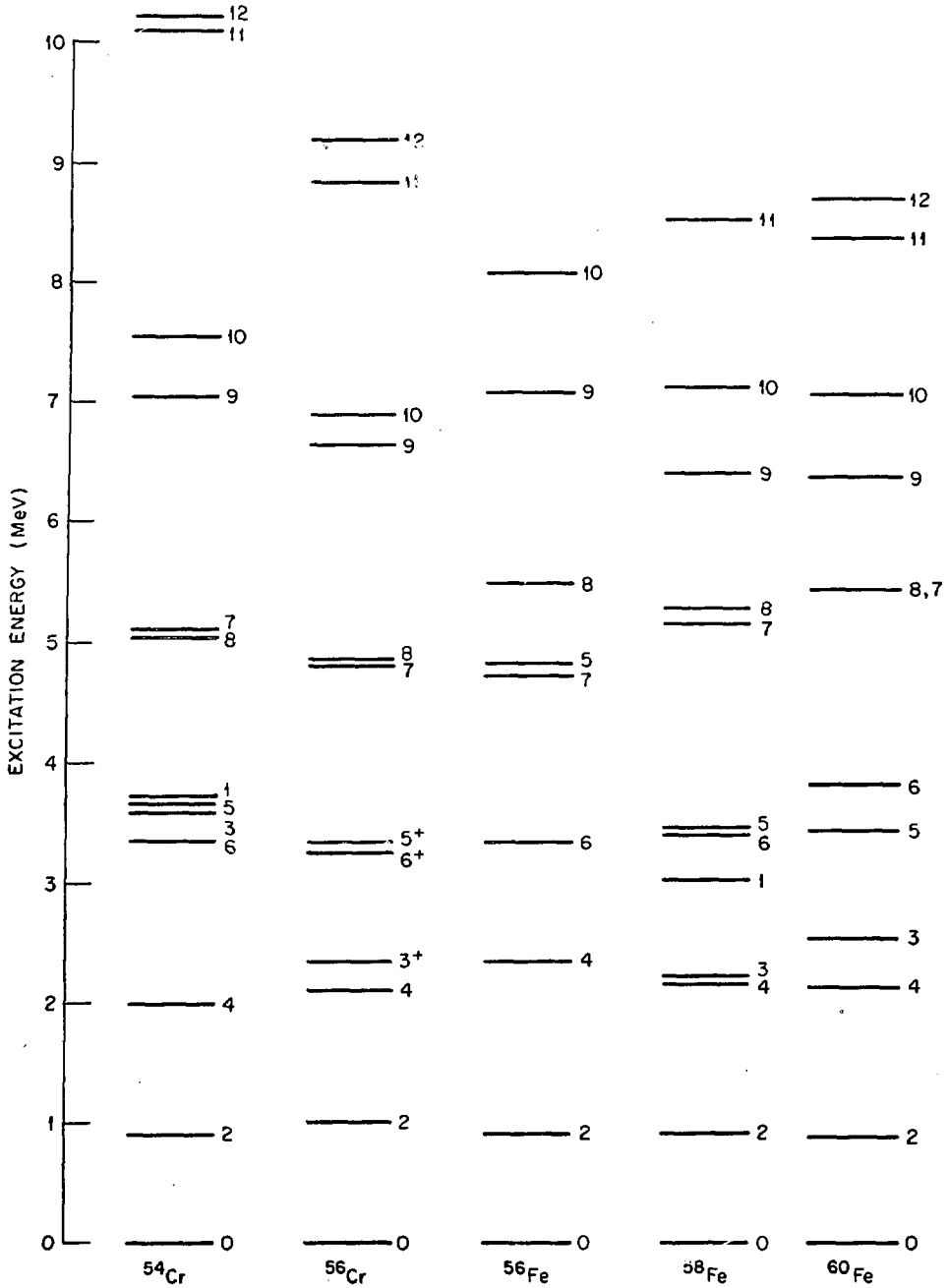

ORNL-DWG 77-13215

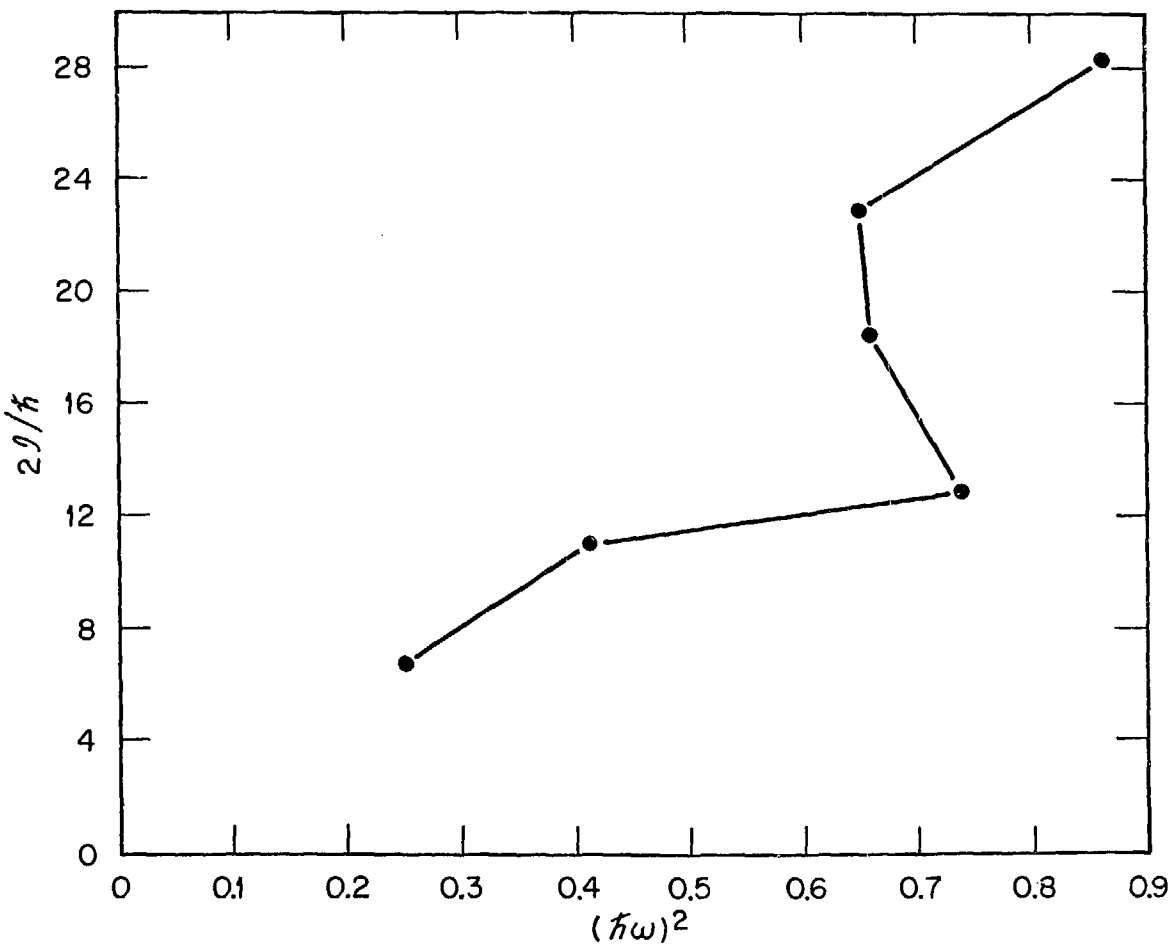

ORNL-DWG 77-13361

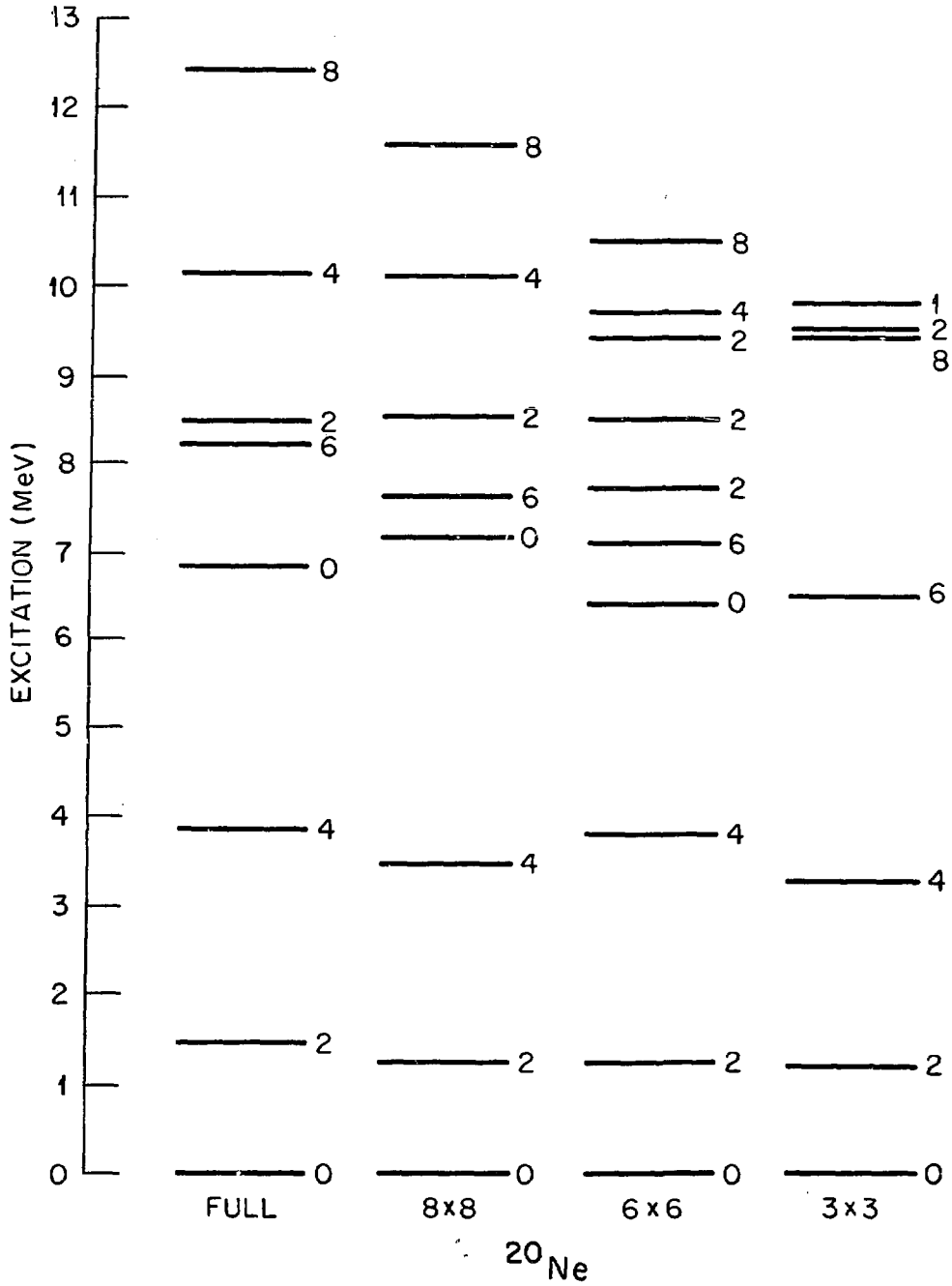
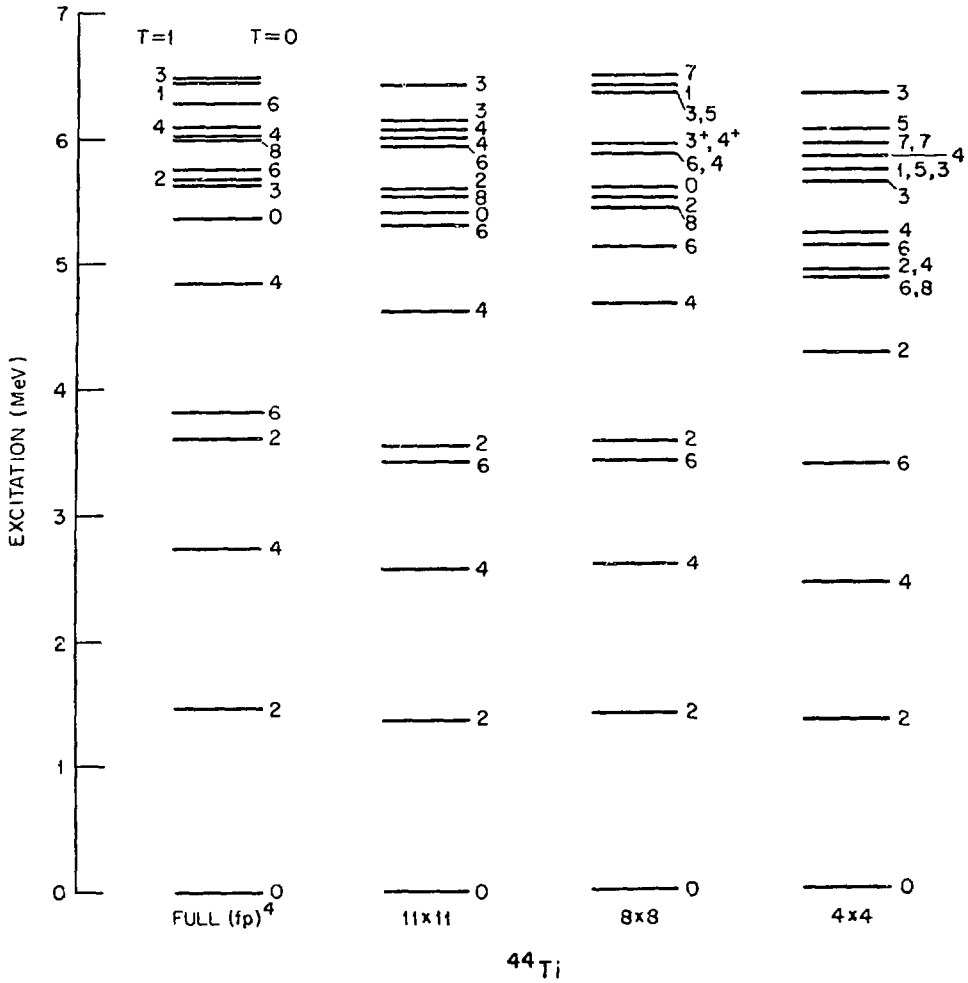
ORNL-DWG 77-13360